

# Dyck Paths, Motzkin Paths and Traffic Jams

**R. A. Blythe**

Department of Physics and Astronomy, University of Manchester, Manchester, M13 9PL, England

**W. Janke**

Institut für Theoretische Physik, Universität Leipzig, Augustusplatz 10/11, 04109 Leipzig, Germany

**D. A. Johnston**

School of Mathematical and Computer Sciences, Heriot-Watt University, Riccarton, Edinburgh EH14 4AS, Scotland

**R. Kenna**

School of Mathematical and Information Sciences, Coventry University, Coventry, CV1 5FB, England

**Abstract.** It has recently been observed that the normalization of a one-dimensional out-of-equilibrium model, the Asymmetric Exclusion Process (ASEP) with random sequential dynamics, is exactly equivalent to the partition function of a two-dimensional lattice path model of one-transit walks, or equivalently Dyck paths. This explains the applicability of the Lee-Yang theory of partition function zeros to the ASEP normalization.

In this paper we consider the exact solution of the *parallel*-update ASEP, a special case of the Nagel-Schreckenberg model for traffic flow, in which the ASEP phase transitions can be interpreted as jamming transitions, and find that Lee-Yang theory still applies. We show that the parallel-update ASEP normalization can be expressed as one of several equivalent two-dimensional lattice path problems involving weighted Dyck or Motzkin paths. We introduce the notion of thermodynamic equivalence for such paths and show that the robustness of the general form of the ASEP phase diagram under various update dynamics is a consequence of this thermodynamic equivalence.

PACS numbers: 05.40.-a, 05.70.Fh, 02.50.Ey

## 1. Introduction

It is a fact of equilibrium statistical-mechanical life that if one wishes to establish the thermodynamics of a model system it is necessary to calculate its partition function. When dealing with *nonequilibrium* stationary states (for example those that carry a current) it is not obvious that the object analogous to the equilibrium partition function, namely the normalisation of the stationary distribution, encodes the thermodynamics in a similar way.

By now the Lee-Yang zeros of the normalisation for a number of nonequilibrium steady states have been studied in the complex plane of the microscopically irreversible transition rates that define a particular model. In particular, various one-dimensional driven diffusive systems [1, 2], reaction-diffusion processes [3, 4, 5] and an urn model for the separation of sand [6] have been investigated and, in each case, the zeros approach the real axis at the appropriate transition points (aspects of this work have been reviewed in [7]). Furthermore, the locus (i.e., impact angle) and density of the zeros near the transition point correspond to the order of the phase transition (defined in physical terms according to whether there is, e.g., phase coexistence or a diverging correlation length) in exactly the same way as for the equilibrium systems long ago considered by Lee and Yang [8, 9]. The various analyses of Lee-Yang zeros for nonequilibrium steady states therefore suggest that the microscopic transition rates somehow play a role similar to equilibrium fugacities.

To some degree this phenomenon can be understood in terms of a graph-theoretic description of the microscopic process [10, 11]. In this picture, one considers a graph in which each vertex corresponds to a microscopic configuration and directed edges to the transitions permitted in an infinitesimal time interval. A representation of the steady-state normalisation can then be shown to coincide with the generating function of spanning in-trees on this graph [12]. Explicitly, if the microscopic transition rates (or, in a discrete-time process, transition probabilities) are drawn from the set  $\{w_1, w_2, \dots, w_N\}$ , the normalisation  $Z$  can be expressed as

$$Z = \sum_{m_1, \dots, m_N} n(m_1, \dots, m_N) w_1^{m_1} w_2^{m_2} \cdots w_N^{m_N}, \quad (1)$$

in which  $n(m_1, \dots, m_N)$  counts the number of spanning in-trees on the graph of configurations with  $m_i$  edges corresponding to a transition that occurs with rate  $w_i$ . Thus the rates  $w_i$  act as fugacities that control the amount to which various classes of spanning in-tree contribute to the overall normalisation. One can see there is the possibility for different classes of trees to dominate the normalisation as the fugacities that weight the trees are varied. One may conjecture that such changes correspond to thermodynamic phase transitions in the microscopic model.

Although this picture is very general, it is also rather abstract. In particular, the relationship between the fugacities and physical observables is unclear. Furthermore, the configuration space is so large (typically exponential in the system size) that it renders formidable the task of connecting the enumeration of trees on the graph of

configurations to its associated physical process.

An insight into the manifestation of nonequilibrium transition rates (generally defined as those that do not satisfy a detailed balance criterion—see e.g. [13]) as equilibrium fugacities was recently provided by Brak *et al.* [11]. In that work the normalisation of the far-from-equilibrium asymmetric simple exclusion process (ASEP) with open boundaries (which was obtained exactly in [14]) was related to the partition function of an equilibrium surface model. In the latter case, the two transition rates associated with the boundaries turn out to be fugacities conjugate to the densities of surface contacts with the horizontal axis from above and below. Thus for this model, there is an interpretation of the normalisation from which the thermodynamics can be extracted using standard equilibrium statistical mechanical techniques.

This result raises the question of whether the relationship between nonequilibrium transition rates and equilibrium fugacities holds for more general nonequilibrium steady states. In this work we investigate this question by revisiting another exactly-solved variant of the ASEP, namely that with *parallel* lattice updates [15, 16]. Whereas the case with a random-sequential updating scheme, referred to above, was introduced to model the kinetics of biopolymerisation [17], the parallel version arises as a special case of the Nagel-Schreckenberg model of traffic flow [18]. From this point of view, the phase transitions in the model's steady state can be related to traffic jamming.

We begin by recalling the definition of the parallel-update ASEP along with some key results. In addition to the two boundary parameters of the random-sequential variant, there is a further quantity,  $p$ , which relates to the degree of parallelism in the dynamics. This gives rise to a normalisation with a considerably more complicated structure than that for the random-sequential ASEP. It is therefore appropriate to check that the Lee-Yang zeros of this normalisation correctly reproduce the known phase behaviour for the model in the complex plane of the defining transition probabilities. This being the case, we move on to establish partition functions for equilibrium surfaces or, equivalently, random walks on two different lattices that have the same thermodynamic phase behaviour as the parallel-update ASEP (and thence jamming in its guise as a traffic model). In each case the extra parameter,  $p$ , generalises the surfaces or walks obtained for the random-sequential ASEP in a physically meaningful way. In one case,  $p$  is a fugacity related to the density of horizontal segments of walks on a triangular lattice and in the other it is related to the density of peaks on the surface. In order to obtain these results we find that it is of great benefit to consider a *grand-canonical* ensemble in which the system size is a quantity exhibiting equilibrium fluctuations about its mean. By considering the general equilibrium thermodynamic properties of the surfaces, we are able to gain a further insight into the robustness of the phase diagram for the ASEP under different microscopic updating schemes.

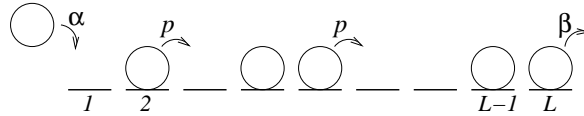


**Figure 1.** Dynamics of the ASEP. The arrow labels indicate the probabilities with which the corresponding transitions occur; site labels are also indicated. Note that the moves are conducted in parallel.

## 2. The Parallel-Update ASEP

The microscopic dynamics of the asymmetric simple exclusion process with parallel dynamics are as shown schematically in Fig. 1 and defined as follows. Particles are introduced with probability  $\alpha$  in each timestep at the start of a one-dimensional lattice with  $L$  sites (if the first site is empty) and leave with probability  $\beta$  at the other end. They can hop with probability  $p$  one unit to the right if that space is empty (or remain still with probability  $1 - p$ ), otherwise if the space to the right is blocked they remain stationary. The update is applied to all particles simultaneously in contrast to the random sequential update scheme. Nevertheless, the latter is recovered in the limit  $p \propto dt \rightarrow 0$  (where  $dt$  is the size of each timestep) if  $\alpha$  and  $\beta$  are rescaled to remain proportional to  $p$ .

The object of interest is the quantity,  $Z$ , that normalises the statistical weight,  $f(\mathcal{C})$ , of lattice configuration,  $\mathcal{C}$ , in the steady state. It is given by

$$Z = \sum_{\mathcal{C}} f(\mathcal{C}) , \quad (2)$$

so that the probability of a configuration  $\mathcal{C}$  is  $P(\mathcal{C}) = f(\mathcal{C})/Z$ . The weights themselves are obtained through the stationarity condition

$$\sum_{\mathcal{C}' \neq \mathcal{C}} [f(\mathcal{C}')W(\mathcal{C}' \rightarrow \mathcal{C}) - f(\mathcal{C})W(\mathcal{C} \rightarrow \mathcal{C}')] = 0 , \quad (3)$$

in which  $W(\mathcal{C} \rightarrow \mathcal{C}')$  is the probability of making the transition from configuration  $\mathcal{C}$  to  $\mathcal{C}'$  in a single timestep. If (3) is solved using Cramer's rule [10], an expression of the form (1) is obtained, with  $\{w_i\}$  forming the set of distinct transition probabilities. Here, this set comprises  $\{\alpha, \beta, p\}$  and their complements  $\{1 - \alpha, 1 - \beta, 1 - p\}$ . The presence of the latter lies in the fact that in one timestep, there is a finite probability that only some subset of the allowed moves is actually performed.

The normalisation for the ASEP with deterministic bulk dynamics ( $p = 1$ ) was obtained using recurrence relations in [15]. Meanwhile, the stochastic case with  $p < 1$  was treated via two different matrix product ansätze [14, 21] that were employed in the independent works of [15] and [16]. Following the notation of [16] we define

$$a_{n,r} = \sum_{t=0}^{n-r} \left[ \binom{n}{r+t} \binom{n-r-1}{t} - \binom{n+1}{r+t+1} \binom{n-r-2}{t-1} \right] (1-p)^t \quad (4)$$

with the conventions  $\binom{X}{0} = 1$  and  $\binom{X}{-1} = 0$  for any integer  $X$ .

This allows the normalisation  $Z_L$  to be expressed as

$$Z_L = Z'_L + pZ'_{L-1}, \quad (5)$$

where

$$Z'_L = \sum_{r=0}^L a_{L,r} \frac{(p(1-\beta)/\beta)^{r+1} - (p(1-\alpha)/\alpha)^{r+1}}{(p(1-\beta)/\beta) - (p(1-\alpha)/\alpha)}. \quad (6)$$

This should be contrasted with the simpler expression for the ASEP with random sequential updates

$$\tilde{Z}_L = \sum_{r=1}^L \frac{r(2L-1-r)!}{L!(L-r)!} \frac{(1/\beta)^{r+1} - (1/\alpha)^{r+1}}{(1/\beta) - (1/\alpha)}, \quad (7)$$

in which  $\alpha$  and  $\beta$  are transition *rates* rather than probabilities.

It is also possible to define *grand-canonical* partition functions [16, 19, 22] by summing over system sizes with fugacity  $z$  in both cases, so that  $\mathcal{Z}_p(z) = \sum_L Z_L z^L$  in the parallel case and  $\tilde{\mathcal{Z}}(z) = \sum_L \tilde{Z}_L z^L$  in the sequential one. These definitions yield

$$\mathcal{Z}_p(z) = \frac{\alpha\beta(1+pz) \left[ 2(1-p)(\alpha\beta - p^2z) - \alpha\beta b^2(1-pz) - \alpha\beta b^2 \sqrt{(1+pz)^2 - 4z} \right]}{2p^4(1-\beta)(1-\alpha)(z - z_{hd})(z - z_{ld})}, \quad (8)$$

where

$$b^2 = \frac{p}{\alpha\beta} [(1-p) - (1-\alpha)(1-\beta)], \quad (9)$$

and

$$z_{ld} = \frac{\alpha(p-\alpha)}{p^2(1-\alpha)}, \quad (10)$$

$$z_{hd} = \frac{\beta(p-\beta)}{p^2(1-\beta)}, \quad (11)$$

in the parallel case [16] and

$$\tilde{\mathcal{Z}}(z) = \frac{4\alpha\beta}{(1-2\alpha - \sqrt{1-4z})(1-2\beta - \sqrt{1-4z})}, \quad (12)$$

in the sequential case [19, 20, 22].

The phase diagram can be extracted by considering the large  $L$  behaviour of  $Z_L$  and  $\tilde{Z}_L$ , either directly or from the asymptotics of the grand-canonical generating functions. In the parallel case using the latter approach [16] we can see that the leading singularities in (8) come from the poles at  $z_{ld}$ ,  $z_{hd}$  in the low- and high-density phases respectively, or from the square root singularity,

$$z_{mc} = \frac{2-p-2\sqrt{1-p}}{p^2}, \quad (13)$$

in the maximal current phase.

The phase diagrams for the random sequential and parallel updates have similar topologies. That for the parallel case is shown in Fig. 2 where the main features to remark upon are the second-order transition lines at  $\alpha$  or  $\beta = 1 - \sqrt{1-p}$  and the first-order line, depicted in bold,  $\alpha = \beta < 1 - \sqrt{1-p}$ . In addition, the mean field solution is

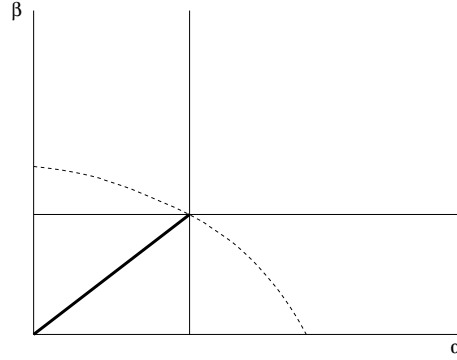


**Figure 2.** Phase diagram of the ASEP with parallel-update dynamics. The second-order lines are at  $\alpha, \beta = 1 - \sqrt{1-p}$  and the first-order line in bold  $\alpha = \beta$  runs from the origin to meet these. Also indicated as a dotted line is the locus  $1-p = (1-\alpha)(1-\beta)$  along which the mean field solution is exact.

exact along the dotted locus  $1-p = (1-\alpha)(1-\beta)$ . The region in which both  $\alpha$  and  $\beta$  are greater than  $1 - \sqrt{1-p}$  is a maximal current phase, that with  $\alpha < 1 - \sqrt{1-p}$  and  $\beta > \alpha$  is a low-density phase, and that with  $\beta < 1 - \sqrt{1-p}$  and  $\alpha > \beta$  is a high-density phase. There are additional transitions within these phases in which the bulk remains the same but the boundary profiles change and these occur at  $\alpha$  or  $\beta = 1 - \sqrt{1-p}$ . In a similar vein the phase diagram for the random sequential updates ASEP shows a maximal current phase for  $\alpha$  and  $\beta > 1/2$  separated from high- and low-density phases by second order transition lines  $\alpha = 1/2, \beta > 1/2$  and  $\beta = 1/2, \alpha > 1/2$ . There, the high- and low-density phases are separated by a first-order line  $\alpha = \beta < 1/2$ .

### 3. Lee-Yang Zeros

It has been observed that, for non-equilibrium systems, a possible equivalent of the reduced free energy might be given by

$$f = - \lim_{L \rightarrow \infty} \frac{1}{L} Z_L. \quad (14)$$

Since for parallel-update dynamics the singularities of (8) determine the asymptotic behaviour of the coefficients  $Z_L$ , we can see that these will simply be given by

$$\begin{aligned} f &= \ln z_{mc}, & \text{for } \alpha, \beta > 1 - \sqrt{1-p}, \\ f &= \ln z_{ld}, & \text{for } \beta > \alpha, \alpha < 1 - \sqrt{1-p}, \\ f &= \ln z_{hd}, & \text{for } \alpha > \beta, \beta < 1 - \sqrt{1-p}. \end{aligned} \quad (15)$$

For random sequential updates the singularities in (12) give

$$\begin{aligned} \tilde{f} &= \ln \frac{1}{4}, & \text{for } \alpha, \beta > 1/2, \\ \tilde{f} &= \ln \alpha(1-\alpha), & \text{for } \beta > \alpha, \alpha < 1/2, \\ \tilde{f} &= \ln \beta(1-\beta), & \text{for } \alpha > \beta, \beta < 1/2, \end{aligned} \quad (16)$$

where  $\tilde{f}$  is similarly defined as  $-\lim_{L \rightarrow \infty} \tilde{Z}_L/L$ .

It has been suggested that for the random sequential update ASEP and other similar non-equilibrium models the Lee-Yang picture of equilibrium phase transitions [8, 9, 23] might still apply [1]. The starting point of Lee and Yang's work was the consideration of how the non-analyticity characteristic of a phase transition appear given that the partition function is a polynomial on finite lattices or graphs. The form of the reduced free energy makes it clear that any non-analyticities are associated with zeros of the partition function when the appropriate fugacities (e.g.  $y = \exp(-2h)$  for a spin model in field) are extended into the complex plane. In general, for a lattice with  $L$  sites, the partition function can be written as a polynomial in the fugacity,

$$Z_L = \sum_r D_r y^r, \quad (17)$$

where the degree of the polynomial is proportional to  $L$ . As the polynomial may be completely expressed in terms of its zeros,  $y_r$ , so too may the (reduced) finite-size free energy:

$$f_L(h) \sim -\frac{1}{L} \ln \prod_r (y - y_r(h)). \quad (18)$$

In the thermodynamic limit,  $L \rightarrow \infty$ , the zeros move in to pinch the real axis at the transition point (or points) and the entire phase structure of the model is determined by their limiting locus and density. From (18), one has

$$f(h) \sim -\int_C dy \rho(y) \ln(y - y(C)), \quad (19)$$

where  $C$  represents some set of curves, or possibly regions, in the complex  $y$ -plane on which the zeros have support and  $\rho(y)$  is the density of the zeros there.

The expressions for the reduced free energy for the ASEP allow a direct determination of the locus of partition function zeros. In general, the partition function zeros delineate the boundaries of different phases since they give the loci along which the free energy is singular, signalling a phase transition. In the Lee-Yang approach one considers an extension to complex parameters, so the free energy,  $f$ , becomes a complex quantity,  $f_l$ , which is the metastable free energy per unit volume in the various phases given by  $l = 1, 2, \dots$ , with  $\text{Re} f_l = f$  characterising the free energy when phase  $l$  is stable. The loci of zeros are then determined by demanding  $\text{Re} f_i = \text{Re} f_j$  for adjacent phases  $i, j$ . Since we have  $f = \ln z_{mc,hd,ld}$  for the various phases of the parallel-update ASEP, we can immediately see that the locus of zeros for the first-order transition will be determined by

$$|z_{hd}| = |z_{ld}|, \quad \alpha, \beta < 1 - \sqrt{1-p}. \quad (20)$$

Substituting in for  $z_{hd}$ ,  $z_{ld}$  from (10) and (11), this gives

$$\left| \frac{\beta(p-\beta)}{p^2(1-\beta)} \right| = \left| \frac{\alpha(p-\alpha)}{p^2(1-\alpha)} \right|. \quad (21)$$

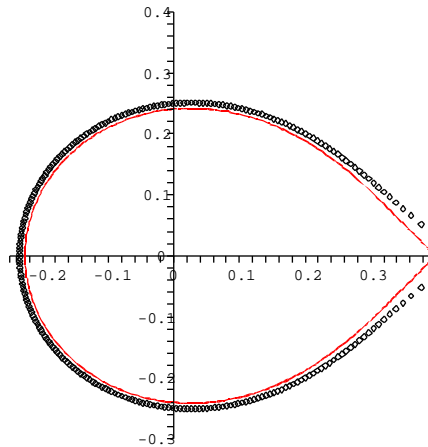


**Figure 3.** The locus of zeros in the complex  $\alpha$ -plane for the parallel-update ASEP with  $p = 16/25$ ,  $\beta = 3/5$ , characteristic of a second-order transition. The diamonds show for comparison numerically determined zeros for a system of size  $L = 250$ .

Similarly, the loci of zeros for the second order transitions are determined by  $|z_{hd}| = |z_{mc}|$  and  $|z_{ld}| = |z_{mc}|$  or, from (10), (11) and (13)

$$\begin{aligned} \left| \frac{\beta(p - \beta)}{p^2(1 - \beta)} \right| &= \left| \frac{2 - p - 2\sqrt{1 - p}}{p^2} \right| \\ \left| \frac{\alpha(p - \alpha)}{p^2(1 - \alpha)} \right| &= \left| \frac{2 - p - 2\sqrt{1 - p}}{p^2} \right|. \end{aligned} \quad (22)$$

These formulae are analogous to those observed in the case of the first-order transition line in random sequential dynamics

$$|\alpha(1 - \alpha)| = |\beta(1 - \beta)|, \quad (23)$$

and for the second order lines

$$|\gamma(1 - \gamma)| = 1/4, \quad (24)$$

where  $\gamma = \alpha, \beta$  depending on the region of the phase diagram.

For definiteness we now consider the zeros of the normalisation for parallel-update dynamics given in (7) with a convenient rational value of  $p = 16/25$ . This places the horizontal and vertical second order transition lines of Fig. 2 at  $\alpha$  and  $\beta = 1 - \sqrt{1 - p} = 2/5$ , respectively. If we consider the former, we can choose a fixed  $\beta$  value, say  $\beta = 3/5$ , which will take us across this line as  $\alpha$  is varied. Substituting  $p = 16/25$ ,  $\beta = 3/5$  into the second of (22) gives the analytic locus of zeros in the complex  $\alpha$ -plane which is plotted in Fig. 3. We have also used (6) to calculate the zeros numerically for system sizes up to  $L = 250$ , and these are plotted in Fig. 3, showing quite good agreement with the limiting analytical results. Similarly we can take a different value of  $\beta$  which crosses the first-order line, say  $\beta = 1/10$ , and use (20) determine the

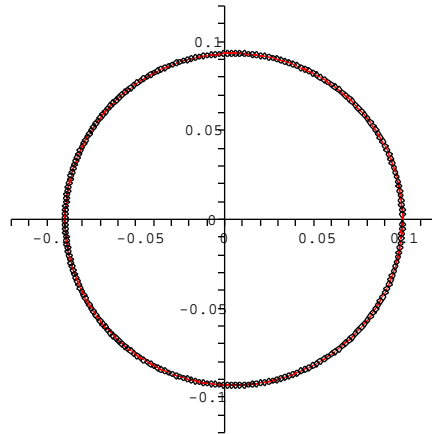


**Figure 4.** The locus of zeros in the complex  $\alpha$ -plane for the parallel-update ASEP with  $p = 16/25$ ,  $\beta = 1/10$  characteristic of a first-order transition. Again numerically obtained zeros for a system of size  $L = 250$  are superimposed.

analytic locus, which is shown in Fig. 4 along with the numerically determined zeros for a system of size  $L = 250$ .

Referring to the discussion of the partition function zeros for the random sequential update ASEP in [2], we thus see the Lee-Yang zeros technique still captures the nature of phase transitions with parallel updates. In Fig. 3 the zeros approach the phase transition point at  $\alpha = 2/5$  at an angle of  $\pi/4$  as might be expected for a second order phase transition. In the first-order case in Fig. 4 the zeros approach the transition point at  $\alpha = \beta = 1/10$  at an angle  $\pi/2$ , which is characteristic of a first-order transition.

It is also possible to look at zeroes of the normalization in the complex  $p$ -plane for given  $\alpha$  and  $\beta$ . In this case one would expect to see a transition at the larger of  $1 - (1 - \alpha)^2$  and  $1 - (1 - \beta)^2$ . The locus of zeroes can be obtained by using, *e.g.*  $|\beta(p - \beta)/(p^2(1 - \beta))| = |(2 - p - 2\sqrt{1 - p})/p^2|$  for fixed  $\beta$  and complex  $p$ . The resulting cardioid locus is shown in Fig. 5, with the transition appearing as the cusp on the real axis.

#### 4. Thermodynamically Equivalent Equilibrium Models

The Lee-Yang analysis of the nonequilibrium normalisation for the parallel-update ASEP in the preceding section suggests that the transition probabilities defining the model are related to equilibrium fugacities. In order to establish the connection concretely, we seek equilibrium models whose partition functions are identical to that of the nonequilibrium normalisation specified by (4)–(6) and in which the parameters  $\alpha, \beta$  and  $p$  are conjugate to physical densities in the equilibrium picture. Such a correspondence was recently provided by Brak *et al.* [11, 25] for the random-sequential

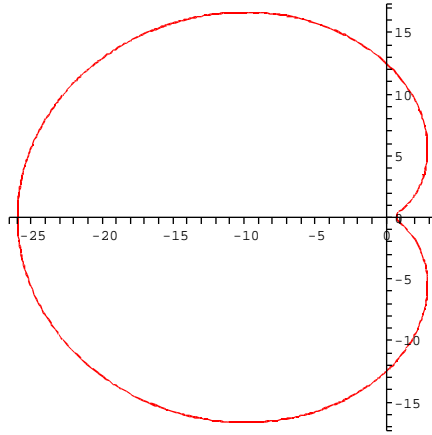


**Figure 5.** The locus of zeros in the complex  $p$ -plane for the parallel-update ASEP with  $\beta = 2/5$ . The transition point is given by the cusp on the real axis at  $1 - (1 - \beta)^2 = 16/25 = 0.64$ .

limit  $p \rightarrow 0$ . Since these equilibrium models have the same phase behaviour as the ASEP, we view them as being *thermodynamically equivalent*.

Our method of choice is to relate the grand-canonical normalisation (8) to generating functions for various types of lattice walks. In an earlier work [19] we demonstrated that in the limit  $p \rightarrow 0$  this approach is technically simpler than transforming the transfer matrices that build up the lattice-path partition functions to the matrix product expressions used to solve the ASEP, which was the method used in [11, 25].

To this end we first note that (8) can be expressed as

$$\mathcal{Z}_p(z) = \frac{\alpha\beta(1 - x_-(z)^2/p)}{(\alpha - x_-(z))(\beta - x_-(z))}, \quad (25)$$

where

$$x_-(z) = \frac{p}{2} \left( (1 + pz) - \sqrt{(1 + pz)^2 - 4z} \right) \quad (26)$$

is one of the roots of the pole terms,

$$z = \frac{x(p - x)}{p^2(1 - x)}, \quad (27)$$

appearing in the grand-canonical partition function.

Let us begin by briefly recapitulating the limit  $p \rightarrow 0$  for which the equilibrium equivalence has been established [11, 19, 25], since the methods we employ will be of utility in the general case. It is clear from (26) that the function  $x_-/p$  remains finite in the limit  $p \rightarrow 0$ . Therefore, to keep (25) finite we write

$$\mathcal{Z}_p(z) = \frac{[\alpha/p][\beta/p](1 - p[x_-(z)/p]^2)}{([\alpha/p] - [x_-(z)/p])([\beta/p] - [x_-(z)/p])}, \quad (28)$$

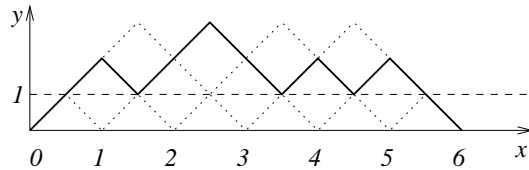


**Figure 6.** An excursion on the rotated square lattice. Note that between the initial and final steps, the excursion comprises sub-excursions away from the line  $y = 1$  and that the length of the path along the  $x$ -axis is equal to the number of up-down pairs.

which indicates the limit  $p \rightarrow 0$  must be taken with  $\alpha/p = \tilde{\alpha}$ ,  $\beta/p = \tilde{\beta}$  as claimed in Section 2. Now note, from (27), that the function  $\tilde{x}_-(z)$  satisfies

$$z = \tilde{x}_-(1 - \tilde{x}_-), \quad (29)$$

in the limit  $p \rightarrow 0$ . This expression implies that  $\tilde{x}_-$  is the generating function of the number of *excursions* on the  $45^\circ$  rotated square lattice, i.e. paths that touch the  $x$ -axis only at the start and end. The fugacity  $z$  is conjugate to the length of the path, measured in terms of the number of pairs of up- and down-steps—see Fig. 6.

The generating function for excursions,  $G_E(z)$ , can be derived by observing from Fig. 6 that each comprises an initial up-step and final down-step (which together contribute a fugacity  $z$ ) between which any non-negative number of excursions away from the line  $y = 1$  can occur. Therefore  $G_E(z)$  can be expanded as

$$G_E(z) = z \left( 1 + G_E(z) + [G_E(z)]^2 + [G_E(z)]^3 + \dots \right) = \frac{z}{1 - G_E(z)}. \quad (30)$$

Comparison with (29) indicates that  $\tilde{x} = G_E(x)$  as claimed.

To complete the path interpretation of (25) in the random-sequential limit, we recast in terms of the rescaled quantities to obtain

$$\tilde{\mathcal{Z}}(z) = \lim_{p \rightarrow 0} \tilde{\mathcal{Z}}_p(z) = \frac{1}{(1 - \tilde{x}_-/\tilde{\alpha})(1 - \tilde{x}_-/\tilde{\beta})}, \quad (31)$$

in agreement with [19, 22]. Expansion of the denominator reveals that this expression describes an ensemble of paths with two sets of excursions, one with a fugacity  $1/\tilde{\alpha}$  per excursion (or, equivalently, return to the  $x$ -axis) and the other with fugacity  $1/\tilde{\beta}$ . For convenience we take the first set of excursions to go above the  $x$ -axis and the second below thus defining a *one-transit walk*, a realisation of which is shown in Fig. 7. In the mathematical literature walks that are constrained to lie on or above the  $x$ -axis are often called *Dyck paths* (see e.g. [26]). A one-transit walk is then a composition of two Dyck paths.

We now use similar methods to establish equilibrium statistical mechanical interpretations for the parallel-update ASEP with general  $p$ .

#### 4.1. Walks on the triangular lattice

Let us now consider excursions on a *triangular* lattice, often called *Motzkin* paths (such as that shown in Fig. 8) in which each horizontal step contributes a fugacity  $u$  and



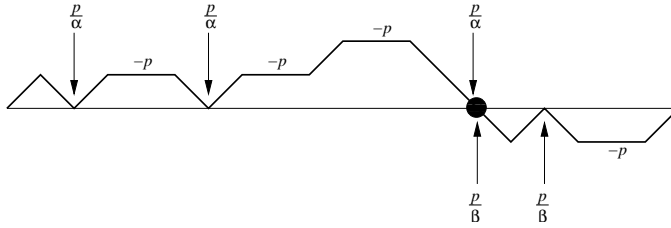


**Figure 9.** A one-transit walk on the triangular lattice with contact weights for the axis. The horizontal segments have a weight  $-pz$  whereas up-down pairs contribute a weight  $z$ , so that the overall power of  $z$  (not shown) is the horizontal length of the path. Meanwhile, there are contact fugacities of  $p/\alpha$  from above and  $p/\beta$  from below.

We remark that only the denominator is relevant in terms of the leading thermodynamic behaviour of the model. Although this will be demonstrated explicitly in Section 5, below, one can see that the factors in the numerator do not alter the location or nature of the singularities in the complex plane. Hence the parallel-update ASEP is thermodynamically equivalent to the one-transit walk on the triangular lattice with fugacities  $p/\alpha$  and  $p/\beta$  associated with contacts from above and below, a fugacity  $z$  conjugate to the path length and a negative fugacity  $-p$  conjugate to the density of horizontal segments as illustrated in Fig. 9.

The origin of the negative fugacity can be understood from the discussions of the Introduction and Section 2. Recall that the normalisation is the generating function of spanning in-trees on the graph of configurations with edges weighted according to the probabilities  $\alpha, \beta, p$  and their complements  $1 - \alpha, 1 - \beta, 1 - p$ . We therefore do not require an expansion of the normalisation in powers  $p$  to have positive coefficients; however, we should expect to find a series expansion in  $p$  and  $q = 1 - p$  with positive coefficients.

One can show this indeed the case for the function  $G_T(-pz, z)$  and thence the expansion of the denominator of (34). Expanding (33) and making the change of variable  $p = 1 - q$  one finds after some routine algebra that

$$G_T(-pz, z) = z \left( 1 + \sum_{n \geq 1} \sum_{m=1}^n \frac{1}{n} \binom{n}{m} \binom{n}{m-1} z^n q^m \right), \quad (35)$$

in which the coefficients of  $z^n q^m$  are clearly positive. The coefficients in (35) are the Narayana numbers [28],

$$N(n, m) = \frac{1}{n} \binom{n}{m} \binom{n}{m-1}, \quad (36)$$

which appear in many combinatorial contexts. Of particular note here is the fact that they are known to count Dyck paths with  $2n$  steps and  $m$  peaks, so this is strongly suggestive that the parallel-update ASEP also admits an interpretation involving standard Dyck paths with weighted peaks. We shall see that this is indeed the case in the next section.

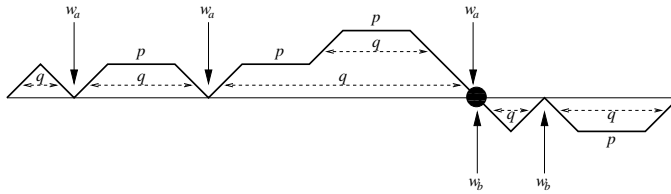


**Figure 10.** An alternative one-transit walk on the triangular lattice. The horizontal segments have a weight  $pz$  whereas up-down pairs contribute a weight  $qz$ . Again the overall (omitted) power of  $z$  is the horizontal length of the path. The contact fugacities from above and below are modified to  $w_a$  and  $w_b$  respectively.

It is also possible to find a triangular lattice path interpretation of the normalisation (25) in which the quantities  $p$  and  $q$  appear more naturally as positive fugacities. To do this, one observes that, since  $p + q = 1$ , (26) can be rewritten as

$$x_-/p - pz = \frac{(1 - pz) - \sqrt{(1 - pz)^2 - 4qz}}{2}. \quad (37)$$

Now the right-hand side of this expression is equal to  $G_T(pz, qz)$ , i.e. the generating function of excursions on the triangular lattice with a fugacity  $p$  associated with each up-down pair and  $q$  with each horizontal step. Expressing (34) in terms of  $G_T(pz, qz)$  yields

$$\mathcal{Z}_p(z) = \frac{1 + (2p/q)G_T(pz, qz) - (p/q)G_T(pz, qz)^2}{(1 - w_a G_T(pz, qz))(1 - w_b G_T(pz, qz))}, \quad (38)$$

with

$$w_a = \frac{p(1 - \alpha)}{q\alpha}, \quad (39)$$

$$w_b = \frac{p(1 - \beta)}{q\beta}. \quad (40)$$

As before, the terms in the numerator of (38) are thermodynamically unimportant. Therefore the phase behaviour of the parallel-update ASEP corresponds to that of a one-transit walk on the triangular lattice with contact fugacities  $w_a$  and  $w_b$  from above and below respectively, as shown in Fig. 10.

In both of the triangular lattice pictures one can understand the limit  $p \rightarrow 0$  intuitively. In this limit, paths with horizontal segments are excluded from the partition function and one recovers the one-transit walks on the rotated square lattice as discussed above.

#### 4.2. Weighted-peak walks on the rotated square lattice

Another natural extension of the one-transit walk on the rotated square lattice that arises in the case of parallel-update dynamics has  $q = 1 - p$  conjugate to the number of *peaks* along the walk. By “peak” we mean here a maximum above the  $x$ -axis, or a minimum below.



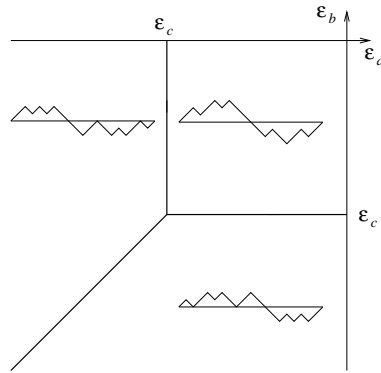


**Figure 12.** Generic phase diagram of a one-transit walk. The density of contacts is nonzero on the side of the axis for which the contact energy  $\epsilon_{a,b}$  is lower. The (negative) critical energy  $\epsilon_c$  at which the entropy of the walk causes it to desorb from the axis depends on  $\epsilon'$  and how it is coupled to the shape of the path.

clearly the robustness of the phase diagram of the ASEP under a variety of updating schemes [30].

Consider a walk of length  $L$  that comprises  $n_a$  excursions above and  $n_b$  excursions below the  $x$ -axis. For added generality we associate with each walk a number,  $m$ , that counts some property that depends on the shape of the walk, but not on whether a particular excursion lies above or below the axis. The number of peaks is such a property. If there is an energy  $\epsilon_a$  ( $\epsilon_b$ ) associated with each of the  $n_a$  ( $n_b$ ) contacts from above (below) and an energy  $\epsilon'$  with the property counted by  $m$ , the free energy of the walk is

$$F = n_a \epsilon_a + n_b \epsilon_b + m \epsilon' - S(L, n_a, n_b, m), \quad (45)$$

in which  $S(L, n_a, n_b, m)$  is the entropy (logarithm of the number of realisations) of paths with fixed  $n_a, n_b$  and  $m$ .

The consequence of  $m$  being independent of whether an excursion lies above or below the axis is that

$$S(L, n_a, n_b, m) = \ln \Omega(L, n_a + n_b, m), \quad (46)$$

where  $\Omega(L, n, m)$  is the number of walks of length  $L$  comprising  $n$  excursions and fixed  $m$ . It then follows that if (45) can be minimised with respect to  $n_a, n_b$  and  $m$  in such a way that  $n = n_a + n_b$  is nonzero, this minimum is achieved by all the excursions being on the side of the  $x$ -axis for which the contact energy is smaller. That is,

$$F = n \min\{\epsilon_a, \epsilon_b\} + m \epsilon' - \ln \Omega(L, n, m). \quad (47)$$

If  $\epsilon_a = \epsilon_b$ , the free energy is neutral to the flipping of an excursion, and so along this coexistence line, the crossing point will wander along the  $x$ -axis. This is suggestive of a first-order phase transition.

It is intuitively clear that the number of possible walks increases as the number of contacts decreases. This implies that once the smaller contact energy has increased

above some critical value, the entropy gained from avoiding the axis (i.e. becoming desorbed) is not offset by any energy saving in contacting the axis. Furthermore, since the free energy depends only on the smaller of contact energies, the critical value must be independent of the larger contact energy. The effect of  $\epsilon'$  will be to favour a particular shape of path, and thus we would expect this to affect the critical contact energy at which the path becomes desorbed. These considerations give rise to a phase diagram with the topology shown in Fig. 12 which is expected to be common to a large class of one-transit walks.

For concreteness, let us now consider the specific case of the peak-weighted walk illustrated in Fig. 11 which has  $m$  as the number of peaks,  $\epsilon_{a,b} = -\ln w_{a,b}$  and  $\epsilon' = -\ln q$ . The number of walks of length  $L$  comprising  $n$  excursions and  $m$  peaks is the coefficient of  $z^L q^m$  in  $[G_P(z, q)]^n$ . This quantity can be obtained readily by applying the Lagrange inversion formula to the functional relation (42) for  $G_P$  [29, 31]. This reveals that for these walks,  $\Omega(L, n, m)$  is the coefficient of  $u^{L-n} q^m$  in

$$\frac{n}{L} \left( q + \frac{u}{1-u} \right)^L,$$

from which one quickly finds

$$\Omega(L, n, m) = \begin{cases} \frac{n}{L} \binom{L}{m} \binom{L-n-1}{m-n} & 0 < n \leq m < L \\ 1 & n = m = L \\ 0 & \text{otherwise.} \end{cases} \quad (48)$$

In the thermodynamic limit,  $L \rightarrow \infty$ , one finds the intensive part of the entropy to be

$$\begin{aligned} s(\rho, \sigma) &= \lim_{L \rightarrow \infty} \frac{1}{L} \ln \Omega(L, \rho L, \sigma L) \\ &= -[\sigma \ln \sigma + 2(1-\sigma) \ln(1-\sigma) + (\sigma - \rho) \ln(\sigma - \rho) - (1-\rho) \ln(1-\rho)] , \end{aligned} \quad (49)$$

in which  $\rho = n/L$  and  $\sigma = m/L$  are the thermodynamic densities of contacts and peaks. Minimising the free energy per unit length

$$f = \rho \min\{\epsilon_a, \epsilon_b\} + \sigma \epsilon' - s(\rho, \sigma), \quad (50)$$

with respect to these densities one finds their equilibrium values are

$$\rho^* = \frac{q(w-1)^2 - 1}{(w-1)(q[w-1] + 1)}, \quad (51)$$

$$\sigma^* = \frac{q(w-1)}{q(w-1) + 1}, \quad (52)$$

for those values of  $q$  and  $w = \max\{w_a, w_b\}$  where the physical requirement  $0 \leq \rho^* \leq \sigma^* \leq 1$  holds. One can check that the inequality  $\rho^* \leq \sigma^* \leq 1$  is automatically true whenever  $\rho^* \geq 0$  is satisfied. The latter condition, however, is violated when  $w_c < 1 + q^{-1/2}$ . Then the free energy is minimised at some point on the boundary of the physical part of the  $(\rho, \sigma)$ -plane. It is easily verified that this point has  $\rho^* = 0$  (i.e. total desorption of the path) and a peak density

$$\sigma^* = \frac{q^{1/2}}{1 + q^{1/2}}. \quad (53)$$

One then finds that in all phases the free energy takes the form

$$f = 2 \ln(1 - \sigma^*) - \ln(1 - \rho^*) . \quad (54)$$

Using these results together with the definitions (39) and (40), one recovers the expressions for the ASEP free energy given in Section 3.

This provides explicit confirmation that the peak-weighted one-transit walk and the parallel-update ASEP are thermodynamically equivalent, despite the fact the grand-canonical partition function of the latter does not agree exactly with that for the ASEP (44) which has additional factors in its numerator. The reason for the equivalence is that these factors describe a small, fixed number of additional excursions which contribute only to the subextensive part of the entropy, and hence become irrelevant in the thermodynamic limit.

## 6. Conclusions

The Lee-Yang theory of partition function zeros has been shown to apply to the ASEP with parallel-update dynamics, correctly pinpointing the first- and second-order transition lines in the model in the complex plane of transition probabilities. This fact suggests that there is an interpretation of these transition rates as equilibrium fugacities. Indeed, we were able to make the correspondence concrete by mapping the normalisation of the ASEP onto partition functions for equilibrium path problems. We found that for parallel updates there were several possible path transcriptions, including two types of adsorbing paths on a triangular lattice and a class of peak-weighted paths on the rotated square lattice. In all cases the appropriate scaling limit recovered the one-transit walk associated with the random sequential update ASEP.

The benefit of finding such mappings is twofold. First one sees quite clearly why a Lee-Yang analysis of a nonequilibrium normalisation should be appropriate in the complex plane of transition rates or probabilities: under the mapping to an equilibrium model, one finds that they *are* fugacities. Secondly, standard techniques from equilibrium statistical mechanics can be used to learn about the thermodynamics of nonequilibrium models. For example, we showed that the structure of the phase diagram for one-transit walks is essentially unchanged when an additional fugacity associated with the shape of the excursions is introduced. In turn, this provides an explanation as to why parallelising the dynamics of the ASEP does not unduly change its phase behaviour. We would therefore expect other variants of the ASEP with a similar phase diagram to be related to one-transit walks at equilibrium. Meanwhile, other nonequilibrium systems are known to be equivalent to equilibrium models (such as the “raise and peel” interface model [32]) so one might expect Lee-Yang theory to apply to these also. Indeed, this does appear to be the case.

In contrast to the case of random-sequential dynamics for the ASEP, we found that the correspondence between the parallel-update ASEP normalisation and a single class of one-transit walks is not exact. This is reflected by the presence of nontrivial

numerator factors in the grand-canonical normalisations (34), (38) and (44). However, as we demonstrated explicitly in Section 5, these factors play no role in the thermodynamics of the ASEP and can essentially be disregarded. Indeed, even for finite-sized systems, the loci of zeros of the normalisation obtained from an “artificial” grand-canonical generating function constructed from the denominator alone are similar to those obtained using the full expressions.

Given that the grand-canonical normalisations for the ASEP with both parallel and random-sequential updates encode the thermodynamics of the models in an extremely compact way, it would be of interest to determine whether there is any method by which these can be calculated *directly* from the microscopic dynamics. Currently, such an enterprise presents a challenge. Therefore, as a first step it would be of interest to investigate other nonequilibrium states for which thermodynamically equivalent equilibrium models have not yet been derived. Chief among these is the partially asymmetric exclusion process (PASEP) [33, 34] in which particles may hop to the left as well as to the right across the lattice. When the left and right hop rates are equal, there is an additional transition to a phase in which there is a zero current in the thermodynamic limit. If one could understand this transition from an equilibrium statistical mechanical point of view, it would give further weight to the growing evidence that phase transitions in equilibrium and nonequilibrium steady states are two sides of same coin.

## 7. Acknowledgements

WJ and DAJ were partially supported by EC network grant *HPRN-CT-1999-00161*. RAB was supported by an EPSRC Fellowship under grant *GR/R44768*.

- [1] P. F. Arndt, Phys. Rev. Lett. **84**, 814 (2000).
- [2] R. A. Blythe and M. R. Evans, Phys. Rev. Lett. **89**, 080601 (2002).
- [3] S. M. Dammer, S. R. Dahmen and H. Hinrichsen, J. Phys. A: Math. Gen. **35**, 4527 (2002).
- [4] F. H. Jafarpour J. Phys. A: Math. Gen. **36**, 7497 (2003).
- [5] F. H. Jafarpour, J. Stat. Phys. **113**, 269 (2003).
- [6] I. Bena, F. Coppex, M. Droz and A. Lipowski, Phys. Rev. Lett. **91**, 160602 (2003).
- [7] R. A. Blythe and M. R. Evans, Braz. J. Phys. **33**, 464 (2003).
- [8] C. N. Yang and T. D. Lee, Phys. Rev. **87**, 404 (1952).
- [9] T. D. Lee and C. N. Yang, Phys. Rev. **87**, 410 (1952).
- [10] R. A. Blythe, *Nonequilibrium Phase Transitions and Dynamical Scaling Regimes*, Ph.D. thesis, University of Edinburgh (2001).
- [11] R. Brak, J. de Gier and V. Rittenberg, J. Phys. A: Math. Gen. **37**, 4303 (2004).
- [12] F. Harary, *Graph Theory* (Addison-Wesley, Reading, Mass., 1969).
- [13] R. A. Blythe and M. R. Evans, Physica A **313**, 110 (2002).
- [14] B. Derrida, M. R. Evans, V. Hakim and V. Pasquier, J. Phys. A: Math. Gen. **26**, 1493 (1993).
- [15] J. de Gier and B. Nienhuis, Phys. Rev. E **59**, 4899 (1998).
- [16] M. R. Evans, N. Rajewsky and E. R. Speer, J. Stat. Phys. **95**, 45 (1999).
- [17] C. T. MacDonald, J. H. Gibbs and A. C. Pipkin, Biopolymers **6**, 1 (1968).
- [18] K. Nagel and M. Schreckenberg, J. Phys. I France **2**, 2221 (1992).

- [19] R. A. Blythe, W. Janke, D. A. Johnston and R. Kenna, “The grand-canonical asymmetric exclusion process and the one-transit walk” [[cond-mat/0401385](#)].
- [20] O. J. Heilmann, *Exact solution of a 1D asymmetric exclusion model with variable cluster size*, to appear in J. Stat. Phys. (2004).
- [21] K. Krebs and S. Sandow, J. Phys. A: Math. Gen. **30**, 3165 (1997).
- [22] M. Depken, *Models of Non-Equilibrium Systems*, D.Phil. thesis, University of Oxford (2003).
- [23] M. E. Fisher, *Lectures in Theoretical Physics*, vol. 7C (University of Colorado Press, Boulder, 1965).
- [24] H. Hinrichsen, Adv. Phys. **49**, 815 (2000).
- [25] R. Brak and J. Essam, J. Phys. A: Math. Gen. **37**, 4183 (2004).
- [26] E. J. Janse van Rensburg, *The Statistical Mechanics of Interacting Walks, Polygons, Animals and Vesicles* (Oxford University Press, Oxford, 2000).
- [27] R. Brak, A. C. Oppenheim and A. L. Owczarek, Int. J. Mod. Phys. B **16**, 1269 (2002).
- [28] T. V. Narayana, Sankhya **21**, 91 (1959).
- [29] E. Deutsch, Discrete Math. **204**, 167 (1999).
- [30] N. Rajewsky, L. Santen, A. Schadschneider and M. Schreckenberg, J. Stat. Phys. **92**, 151 (1998).
- [31] H. S. Wilf, *Generatingfunctionology* (Academic Press, San Diego, 1994).
- [32] J. de Gier and B. Nienhuis, J. Stat. Phys. **114**, 1 (2004).
- [33] T. Sasamoto, J. Phys. A: Math. Gen. **32**, 7109 (1999).
- [34] R. A. Blythe, M. R. Evans, F. Colaiori and F. H. L. Essler, J. Phys. A: Math. Gen. **33**, 2313 (2000).